fermentation

MDPI

Article

Biomethane Potential in Anaerobic Biodegradation of Commercial Bioplastic Materials

Zsuzsanna Üveges [1], Mariem Damak [1,2], Szandra Klátyik [1], Muhammad Wajahat Ramay [1], György Fekete [1], Zsolt Varga [1], Csaba Gyuricza [3], András Székács [1,4] and László Aleksza [1,2,*]

[1] Institute of Environmental Sciences, Hungarian University of Agriculture and Life Sciences, Páter Károly u. 1, H-2100 Gödöllő, Hungary
[2] Profikomp Environmental Technologies Inc., Kühne Ede u. 7, H-2100 Gödöllő, Hungary
[3] Institute of Agronomy, Hungarian University of Agriculture and Life Sciences, Páter Károly u. 1, H-2100 Gödöllő, Hungary
[4] Agrotechnology National Laboratory, Hungarian University of Agriculture and Life Sciences, Páter Károly u. 1, H-2100 Gödöllő, Hungary
* Correspondence: aleksza.laszlo@uni-mate.hu; Tel.: +36-28-512-490

Abstract: Bioplastics have emerged as a promising alternative to conventional plastics, marketed as environmentally friendly and sustainable materials. They provide a variety of methods for efficient waste management contributing to the goals of the circular economy. At their end-of-life stage, bioplastics can generate added value through aerobic and anaerobic biological treatments (composting or anaerobic digestion). In this study, biomethane potential (BMP) tests were carried out under mesophilic conditions on eight different catering biodegradable plastics available in the market and certified as being biodegradable under industrial composting conditions. Chemical analysis of the biodegradable plastics included elemental analysis, Fourier-transform infrared spectroscopy, and inductively coupled plasma–optical emission spectrometry. Key differences were observed in total solids (TS) and volatile solids (VS) contents between the studied biopolymer products. TS values ranged between 85.00 ± 0.26% (Product 8) and 99.16 ± 0.23% (Product 4), whereas VS content ranged between 64.57 ± 0.25 %wm (Product 6) and 99.14 ± 0.17 %wm (Product 4). Elemental analysis (elements C, H, N, S, and O) was used to estimate the theoretical methane production (ThBMP) of each product. The highest ThBMP (538.6 ± 8.7 NmL/gVS) was observed in Product 4 correlated with the highest C and H contents, while the lowest ThBMP (431.8 ± 6.1 NmL/gVS) was observed in Product 2. Significant differences were recorded between BMP values according to the chemical composition of the polymers. The average of BMP values ranged between 50.4 ± 2.1 NmL/gVS and 437.5 ± 1.0 NmL/gVS. Despite being characterized by the same composition (cellulose/cellulose derivatives and calcium carbonate), Products 2, 3, and 6 revealed significant differences in terms of TS, VS, ThBMP, and BMP. Furthermore, a significant statistical relationship ($p < 0.001$) was found between time (days) and BMP values of the eight products (R^2 = 0.899–0.964) during the initial phase. The study confirmed that cellulose-based materials can convert efficiently under mesophilic conditions into methane, at a relatively short retention time; hence, they can be regarded as a promising material for co-digestion with feedstock in industrial anaerobic biogas plants. In contrast, biodegradation of polylactic acids (PLA) does not occur under mesophilic conditions, and hence, pre-treatment of the polymers is recommended. Moreover, PLA-containing products are highly affected by the presence of other components (e.g., polybutylene adipate terephthalate and cellulose/cellulose derivatives).

Keywords: biodegradable plastic; anaerobic digestion; biomethane potential; cellulose; PLA/PBAT; FT-IR spectroscopy; elemental analysis

Citation: Üveges, Z.; Damak, M.; Klátyik, S.; Ramay, M.W.; Fekete, G.; Varga, Z.; Gyuricza, C.; Székács, A.; Aleksza, L. Biomethane Potential in Anaerobic Biodegradation of Commercial Bioplastic Materials. *Fermentation* **2023**, *9*, 261. https://doi.org/10.3390/fermentation9030261

Academic Editor: Alessio Siciliano

Received: 16 January 2023
Revised: 28 February 2023
Accepted: 2 March 2023
Published: 6 March 2023

1. Introduction

Over the past decade, massive amounts of conventional plastics have been extensively produced and disposed of. Their low cost, versatility, and chemical properties have led to

an estimated annual production of 357 million tonnes [1]. Plastics are synthetic or semi-synthetic carbon-based polymers, 99% of which are produced from non-renewable carbon sources such as petroleum derivatives [2], and are characterized by their resistance to degradation in nature as they are composed of inert, hydrophobic, high-molecular-weight long-chain polymers [3]. The prolonged half-life of plastics, their excessive use, and their poor end-of-life management have led to serious environmental issues affecting the quality of human life, wildlife, and ecosystems [4]. Bioplastics have emerged as a promising alternative to conventional plastics, marketed as environmentally friendly and sustainable materials. They provide a variety of methods for efficient waste management contributing to the goals of a circular economy. At their end of life, bioplastics can generate added value through aerobic and anaerobic biological treatments (composting or anaerobic digestion).

Because of their biocompatibility and biodegradability, bioplastics are regarded as superior polymers to synthetic plastics, making them ideal for applications in packaging, biomedical, and other value-added industrial applications [4]. Table 1 summarizes the main differences between conventional plastics and bioplastics.

As reported by the organization European Bioplastics, biopolymers can be classified into three categories based on their resources and biodegradability: (1) bio-based and biodegradable, (2) bio-based but not-biodegradable, and (3) biodegradable plastics that do not come from renewable energy sources [1]. The term bio-based refers to the renewable resources such as proteins and lipids from which these materials are produced [5]. Rice, corn, tapioca, potatoes, soybeans, wood cellulose, wheat fiber, and bagasse are among the feedstock utilized in the manufacturing of bioplastics [6]. On the other hand, the term "biodegradation" refers to a mineralization process mediated by a wide variety of microorganisms at the end-of-life stage of biopolymers. The biodegradation process is affected by (1) abiotic environmental factors such as pH, temperature, and moisture, (2) biotic factors such as the types of enzymes present during the biodegradation process, and (3) polymer characteristics such as crystallinity, type of functional groups, and molecular weight [7–9].

Plastics that disintegrate by oxidative abiotic processes are termed oxo-degradable. Such decomposition can be facilitated by incorporating pro-oxidants (e.g., transition metal compounds) within the plastic formula. It is very important to clarify that oxo-degradable plastics are conventional plastics that rapidly disintegrate in the environment upon exposure to light, heat, or mechanical pressure, yet these materials do not biodegrade, only break down into smaller fragments (microplastics and nanoplastics). Therefore, they cannot be considered as biodegradable, unless their abiotic oxidative disintegration is followed by biotic decomposition. In the latter case, abiotic fragmentation can actually favorably affect subsequent microbial decomposition. These special oxo-degradable polymers that subsequently undergo oxidative microbial decomposition are termed oxo-biodegradable. However, again, oxo-degradability is not at all a guarantee for biodegradability, and the vast majority of oxo-degradable plastics are persistent environmental pollutants. In turn, the use of oxo-degradable plastics is already restricted or banned in numerous countries (e.g., the European Union, Switzerland, and New Zealand), due to the related environmental problems, microplastic production, inability to be recycled, and impurities in composts.

Based on data from the European Bioplastics Association [1], currently, bioplastics represent less than one percent of the total plastics production capacities. Global bioplastic production was 1792 thousand tonnes and 2217 thousand tonnes in 2021 and 2022, respectively (Figure 1). However, as the demand is increasing, and with more sophisticated biopolymers, applications, and products emerging, the market for bioplastics is continuously growing and diversifying. Global bioplastic production is estimated to reach 6291 thousand tonnes in 2027 (Figure 1). The manufacturing of biodegradable plastics, such as polylactic acids (PLAs), polyhydroxyalkanoates, starch blends, and others, accounts for more than 64% of the world's bioplastic capacities [1]. On the other hand, bio-based, non-biodegradable plastics altogether make up about 36% of global bioplastics production capacities [1]. Furthermore, as anticipated by the association, the production of biodegrad-

able plastics would nearly triple to 5.3 million tonnes in 2026, due to the rapid development of polymers such as polybutylene adipate terephthalate (PBAT) and polybutylene succinate, as well as the constant increase in PLA production.

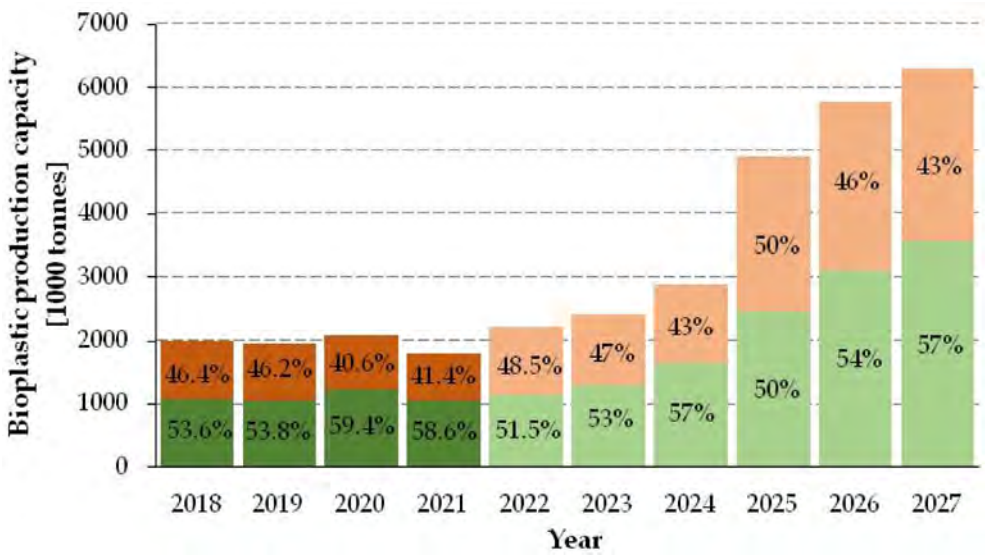

Figure 1. Global production capacities of bioplastics. Biodegradable bioplastics (green columns) and bio-based, non-biodegradable plastics (brown columns). Dark and pale colors indicate actual and forecasted data, respectively. Different numbers in the columns indicate percentage ratios between the two categories. Data reported by the European Bioplastics Association [1].

Anaerobic digestion (AD) is a complex microbial process that turns biomass into biogas in the absence of oxygen [10,11]. It is a common method for treating organic waste, and it is regarded as the most favorable alternative for the valorization of biowaste from an environmental point of view as compared to incineration, sanitary landfill, and deposition [10,12,13]. The AD process takes place through four distinguished steps: hydrolysis, acidogenesis, acetogenesis, and methanogenesis. By the end of the last step, the biomass is converted into biogas (mainly a mixture of CH_4 and CO_2) and digestate. Several anaerobic microorganisms are implicated in the anaerobic digestion process. Both facultative and obligate anaerobic bacteria make up the microorganisms that are responsible for the processes of hydrolysis, acidogenesis, and acetogenesis, namely, *Clostridium* spp., *Peptococcus* anaerobes, *Lactobacillus*, *Actinomyces*, and *Escherichia coli.* [14]. Furthermore, the methanogens responsible for methane generation belong to the Archaea domain, classified as slow-growing microorganisms and particularly oxygen-sensitive such as *Methanobacteria*, *Methanosarcina*, and *Methanothrix* [14,15].

On the one hand, biogas can be utilized as a green energy source to generate heat, electricity, and fuel for vehicles [16–18]. After biogas upgrading, biomethane can be injected into the natural gas grid since it has the same properties as natural gas, notably in terms of heating value [16,19]. On the other hand, the digestate is rich in bioavailable nutrients and organic matter, which makes it suitable for agricultural use as a fertilizer for plants and as a soil amendment [20,21].

The majority of biodegradable polymers that decompose in industrial composting conditions also degrade under AD circumstances [6]. The anaerobic biodegradability examination of different biopolymers is strongly dependent on environmental conditions; therefore, different standards are devised, simulating different conditions where anaerobic biodegradation of bioplastics can occur, such as MSZ EN 13432, ISO 11734, ISO 14853, ISO 15985, ASTM D5210-92, ASTM D5511-02, ASTM D5526-94D [22–28]. Anaerobic biodegradability of bioplastics can also be assessed by measuring particular methane production by the test material using biomethane potential (BMP) testing [29,30]. It is a reliable and inexpensive method for determining the amount and rate at which organic matter is converted

into methane and is an essential step to optimize the AD [31]. The determination of BMP of a certain substrate before feeding it to a full-scale AD facility can be utilized to optimize environmental factors (such as temperature, organic loading rate, digester capacity, etc.) and methane production of the converted organic matter [31]. In the last few years, a number of studies about biomethane potential (BMP) tests have been carried out to demonstrate biodigestibility, methane yield, reaction-rate kinetics, the extent of anaerobic activity, the influence of pretreatment, and the effects of mixing different viscosities [12]. Numerous types of substrates have been used, including solid household trash, pulp and paper mill sludge, wastewater sludge, commercial food waste, livestock materials (manures), agricultural wastes, plant leftovers and different types of bioplastics [12]. Moreover, BMP tests are easy to carry out [30]. They are accomplished by feeding a specified amount of an organic substrate to an active anaerobic inoculum in an airtight bottle, where the biogas generated is measured, and its methane concentration is estimated. Additionally, a BMP laboratory test is still the most reliable approach for determining the methane production of a specific substrate [31]. This test is easier than full-scale applications and facilitates the commercialization of anaerobic digesters.

Table 1. Main differences between conventional plastics and bioplastics.

Characteristics	Conventional Plastics	Bioplastics
Materials	Produced from non-renewable resources such as fossil fuel and natural gas.	Commonly produced from renewable biomass resources or biodegradable fossil-based resources.
Greenhouse gas emissions	High greenhouse gases emissions such as carbon dioxide (CO_2). Plastics account for 3.4% of global greenhouse gas emissions.	Significantly lower greenhouse gas emissions than traditional plastics over their lifetime [16].
Biodegradability	Most conventional plastics are not biodegradable, such as polyethylene, polypropylene, polystyrene, poly(vinyl chloride), and poly(ethylene terephthalate).	Most of the bioplastics are biodegradable depending on their chemical and physical structure.
End-of-life options	- Recycling: only 9% of global plastic waste is recycled. - Incineration: 19% of global plastic waste is incinerated. - Landfilling: 50% is disposed of in landfills. - Littering: 22% ends up in uncontrolled dumpsites, open pits, or terrestrial or aquatic habitats.	- Composting - Anaerobic digestion
Circularity	Circularity is not guaranteed.	Organic recycling involves closing the loop by creating a new resource (compost, biogas) that can be utilized to grow additional plants.

This study aims to understand the anaerobic biodegradation behavior under mesophilic conditions of commercially available biodegradable plastic materials which are certified according to MSZ EN 13432 [22] as biodegradable under industrial composting conditions and represent raw materials for cutlery and tableware manufacturing used in food restaurants, canteens, and festivals. Furthermore, the organic portion consisting primarily of food waste is the most significant municipal waste stream. Biodegradable and compostable products may improve organic waste management, allowing for cleaner organic flow collection and value addition from their aerobic and anaerobic treatment. As catering industry waste can enter mesophilic AD plants, this study intends to examine the performance of catering waste at its end-of-life stage by evaluating its methane potential under mesophilic conditions, and hence, this study aims to provide information on which materials show good performance at these conditions and which materials are to be avoided or pre-treated before entering AD plants. Finally, this study aimed to evaluate the effect of chemical composition and additives on the BMP of different commercially available bioplastics and to enable a comparison between biodegradation of biopolymers under anaerobic mesophilic conditions.

2. Materials and Methods

2.1. Biodegradable Biopolymers

The plastics used in our study are eight different catering biodegradable polymers available in the market and certified as being biodegradable under industrial composting conditions (EN 13432) [22]. The bioplastic samples were black-box samples, produced under trades names but their chemical composition were not given by the provider; hence, it was unknown by the beginning of the experiment. The samples represent raw materials for cutlery and tableware manufacturing used in food restaurants, canteens, and festivals. These products can enter the AD plants as they are certified to be biodegradable under industrial composting conditions. Samples are labeled with sequential numbers as Product 1 to Product 8. Product 1 to 7 were films, whereas Product 8 was a plate.

2.2. Inoculum

The mesophilic inoculum used for the AD process in this study was obtained from the mesophilic reactor of an operating plant in Hungary (Solti Biogaz Ltd., Solt, Hungary). The substrates of this plant are agricultural materials (animal manure and plant residue) and industrial food by-products.

2.3. Chemical Analysis

Chemical analysis of the biodegradable plastics used in the study included elemental analysis, Fourier-transform infrared spectroscopy (FT-IR), and inductively coupled plasma–optical emission spectrometry (ICP-OES). Elemental analysis was performed with an Elementar Vario Macro Cube analyzer (Elementar Analysensysteme Gmbh., Langenselbold, Hesse, Germany). FT-IR spectroscopy was performed using a Bruker Tensor 27 spectrophotometer (Bruker Corp., Billerica, MA, USA) equipped with a monolithic diamond accessory in attenuated total reflection (ATR) mode. The spectra were obtained within the frequency range of 4000–500 cm^{-1} with spectral resolution of 4 cm^{-1}. ICP-OES was performed on a Thermo Scientific iCAP 6500 Duo View (Thermo Fisher Scientific, Cambridge, UK).

2.4. Rate of Biodegradation

Various parameters were monitored and calculated during the decomposition study of the biodegradable plastics. Thus, levels of total solid (TS), volatile solids (VS), and organic matter (OM) were determined and expressed as a percentage of the wet mass (wm). In addition, elemental composition was determined for carbon (C), hydrogen (H), nitrogen (N), sulfur (S), calcium (Ca), and magnesium (Mg) content, and it was expressed as a percentage of the dry mass (dm). The parameters measured or calculated and the methods used for the analysis are summarized in Table 2.

Table 2. Measured physicochemical parameters during the study.

Parameter Measured	Description	Test Method
TS	Total solids	Mass measurement, MSZ EN 13040:2008 [32]
VS	Volatile solids	Standard measurement for examination of water and wastewater (APHA, 2005) [33]
OM	Organic matter	Loss on ignition (MSZ EN 15935:2013) [34].
pH	Acidity	Potentiometric determination of H^+ ion concentration, MSZ EN 13037:2012 [35]
CHNS	Carbon (C), hydrogen (H), nitrogen (N), and sulfur (S) content	Elemental analysis to measure the conversion of carbon (C) to methane (CH_4) (biodegradability%) MSZ EN ISO 16948:2015 [36] MSZ EN ISO 16994:2017 [37]
Ca	Calcium [HNO_3/H_2O_2]	Inductively coupled plasma–optical emission spectrometry (ICP-OES) MSZ 21470-50:2006 [38]
Mg	Magnesium [HNO_3/H_2O_2]	Inductively coupled plasma–optical emission spectrometry (ICP-OES) MSZ 21470-50:2006 [38]

The extent of the rate of biodegradation (BD) was estimated by comparing the experimental BMP and the theoretical BMP (ThBMP) (Equation (1)) [4]:

$$\text{BD } (\%) = \frac{\text{Experimental biomethane production}}{\text{Theoritical biomethane prodcution}} \times 100 \quad (1)$$

Each plastic used in this experiment was characterized with regard to TS, VS, pH, and elemental analysis (carbon, hydrogen, nitrogen, and sulfur). TS measurement was executed based on the standard MSZ EN 13040:2008 [32]. Measurements of VS were performed by the standard measurement APHA, 2005 [33]. OM values were based on the method of loss on ignition (LOI) (MSZ EN 15935:2013) [34]. pH was measured according to the standard MSZ EN 13037:2012 [35].

The O content was estimated by the difference between the VS, carbon, hydrogen, nitrogen, and sulfur [11]. A quantitative link between an organic component and its by-products following AD can be estimated through mass balance. Hence, Boyle's (1977) [39] equation (Equation (2)) was used to estimate the theoretical methane production of each plastic product. The equation is based on the general chemical reaction of microbial AD converting an organic substance with optional elemental composition ($C_xH_yO_zN_nS_s$). The stoichiometrically necessary amounts of water (H_2O) to methane (CH_4), carbon dioxide (CO_2), ammonia (NH_3), hydrogen sulfide (H_2S), and the amount of availability of each element in the organic substance are taken into consideration. Thus, theoretical methane production, as a function of the elemental composition of the organic substance, is expressed (Equation (2)):

$$\nu_{CH_4}(C_xH_yO_zN_nS_s) = \frac{\frac{x}{2} + \frac{y}{8} - \frac{z}{4} - \frac{3n}{8} - \frac{s}{4}}{12x + y + 16z + 14n + 32s} \times 22.4 \quad (2)$$

where ν_{CH_4} is the specific volume (normalized L per g) of methane generated from one mole of the organic substance.

2.5. Biomethane Potential (BMP) Test

The AD test was carried out in an Automatic Methane Potential Test System II instrument (BPC Instruments AB, Lund, Sweden). The system consisted of a water bath with 15 reactors of 600 mL each connected to a mechanical agitator, and an alkali solution unit for chemically removing CO_2 and H_2S. The remaining gas after scrubbing was transported to the subsequent gas flow meter with 15 parallel cells, one for each reactor. Data was then recorded by the data acquisition system.

Before the tests, the BMP reactors were purged with high-purity nitrogen for 3 min to remove oxygen from the reactor head space. The exact weights of the substrates and the inoculum were calculated by a built-in Automatic Methane Potential Test System II instrument software (BPC Instruments AB, Lund, Sweden), based on the VS and the inoculum-to-substrate ratio (I/S), the latter always being 2:1. The total volume of the substrate and the inoculum in the reactors was always 400 mL; therefore, the volume of the gas that was produced was 200 mL.

Blank and positive controls were measured in every sequence in triplicate parallel tests, and plastic product samples were also arrayed in 3-3 parallels. Microcrystalline cellulose purchased from Molar Chemicals Ltd. (Halásztelek, Hungary) was used as a positive control with a known BMP (350 ± 29 NmL of methane/gVS) [40] to verify the experimental setup and execution, as well as the inoculum's performance. The test was validated only when the BMP of the positive control was within the predicted range. In the case of the blank control, only inoculum was placed in the reactors. The positive control served as a reference with regard to identifying the biological activity of the inoculum. The methane produced from the blank control was subtracted from the production of other bottles and evaluated per gram of VS added. The normalized BMP (expressed in units of

mL volume under normal conditions per gram of volatile solid, NmL/gVS) was calculated using the following equation (Equation (3)) [41]:

$$\text{BMP} = \frac{\nu S - \nu B \times \frac{m_{IS}}{m_{IB}}}{m_{VS}} \quad (3)$$

where νS is the accumulated volume (normalized mL, NmL) of methane produced from the sample (i.e., inoculum and organic substance) in the reactor, νB is the accumulated volume of methane (normalized mL, NmL) produced from the blank (inoculum only) in the reactor, m_{IS} is the total amount (g) of inoculum in the sample, m_{IB} is the total amount (g) of inoculum in the blank, and m_{VS} is the mass of the volatile solid organic substance in the sample (gVS). BD rates were calculated as percentage quotient of BMP and ThBMP (see Section 2.4). The length of time for one sequence was 30 days [42], and BD at the end of test period (biodegradability rate after 30 days, BD_{30}) were used for comparative analysis.

2.6. Statistical Analysis

Statistical analyses were conducted using the R Statistical program 4.2.1. (R Development Core Team, Vienna, Austria). During the elemental analysis and BMP test, all measurements were carried out in three replicates for each investigated bioplastic material, including blank and positive controls. Differences in the measured parameters of elemental analysis, as well as the BMP values determined weekly and on the last day (30th day) of the experiment, were analyzed with the use of general linear models according to the various investigated commercial bioplastic materials. The significance of the differences between the measured and theoretical BMP values was tested with the use of paired t-tests at the significance level of 0.05. Before statistical analysis, the normality of the data and the homogeneity of variance were also checked by Shapiro–Wilk and Levene's or Bartlett's tests. Furthermore, the applicability of the fitted model was checked in each case with diagnostic plots (residual variances, QQ plot, Cook's distance plot). Tukey's honest significant difference (HSD) tests were conducted as post hoc analyses to assess the significant differences between groups. The effects of the time and chemical composition on BMP values, as well as their interactions, were also investigated. In cases where the conditions for the application of the chosen statistical method were not met, the non-parametric Kruskal–Wallis test was performed.

During the analysis of BMP curves, the initial phase of the curves was evaluated by linear regression, but polynomial regression calculations were also conducted on BMP curves. The best polynomial regression fitting (second, third, or fourth order) was selected based on the statistical comparison of the models, and with the use of the Akaike Information Criterion (AIC) values.

Various mathematical functions have been used in the scientific literature to model the potential and rate of biogas (e.g., methane) production, among which the Gompertz models, especially the modified Gompertz model, are commonly used for the modeling of BMP [43–47]. Although originally developed for demography modeling in the 19th century, the Gompertz model gained utility in that it has been modified for assessing microbial growth, and the main advantage of the approach is that it allows asymmetric asymptotic fitting at the lower (initiation) and upper (saturation) plateaus. Thus, the Gompertz model and the modified Gompertz model can be described for BMP as functions of time (t) in the mathematical forms below (Equations (4) and (5), respectively):

$$\text{BMP} = \text{a} \times \text{e}^{-\text{e}^{(\text{b}-\text{c}\times\text{t})}} \quad (4)$$

where a is the estimated maximum value of the BMP (normalized mL per gram of volatile solid, NmL/gVS), e is Euler's function (e = 2.7183), b is shift along the time axis (analogous to the lag phase), c is the slope of the curve at the infection point [48], and

$$\text{BMP} = \text{A} \times \text{e}^{-\text{e}^{\left(\frac{\mu_m \times \text{e}}{\text{A}}(\lambda - \text{t}) + 1\right)}} \quad (5)$$

where A is the estimated maximum value of the BMP (normalized mL per gram of volatile solid, NmL/gVS), e is Euler's function (e = 2.7183), μ_m is the maximum specific methane production (normalized mL per gram of volatile solid per day, NmL/gVS/day), and λ is the lag phase (day) [44,45,49].

Therefore, the results of BMP tests were modeled by the traditional Gompertz and modified Gompertz models with the use of nls() function of the R Statistical program 4.2.1. (R Development Core Team, Vienna, Austria). After the fit of the basic Gompertz curve to the experimental BMP data, coefficients a, b, and c, as well as A, μ_m, and λ, were interpreted and evaluated. The goodness of fit of the models was checked and compared based on the determined R^2 values.

3. Results and Discussion

3.1. Chemical Analysis

The chemical composition of each plastic product was examined by FT-IR spectroscopy, elemental analysis, and ICE-OEP. Visual analysis of the polymer films revealed differences in the appearance of each side of some of them; therefore, FT-IR spectroscopy was performed on both sides of each film. Figure 2 shows the FT-IR spectra of each plastic from Product 1 to Product 8.

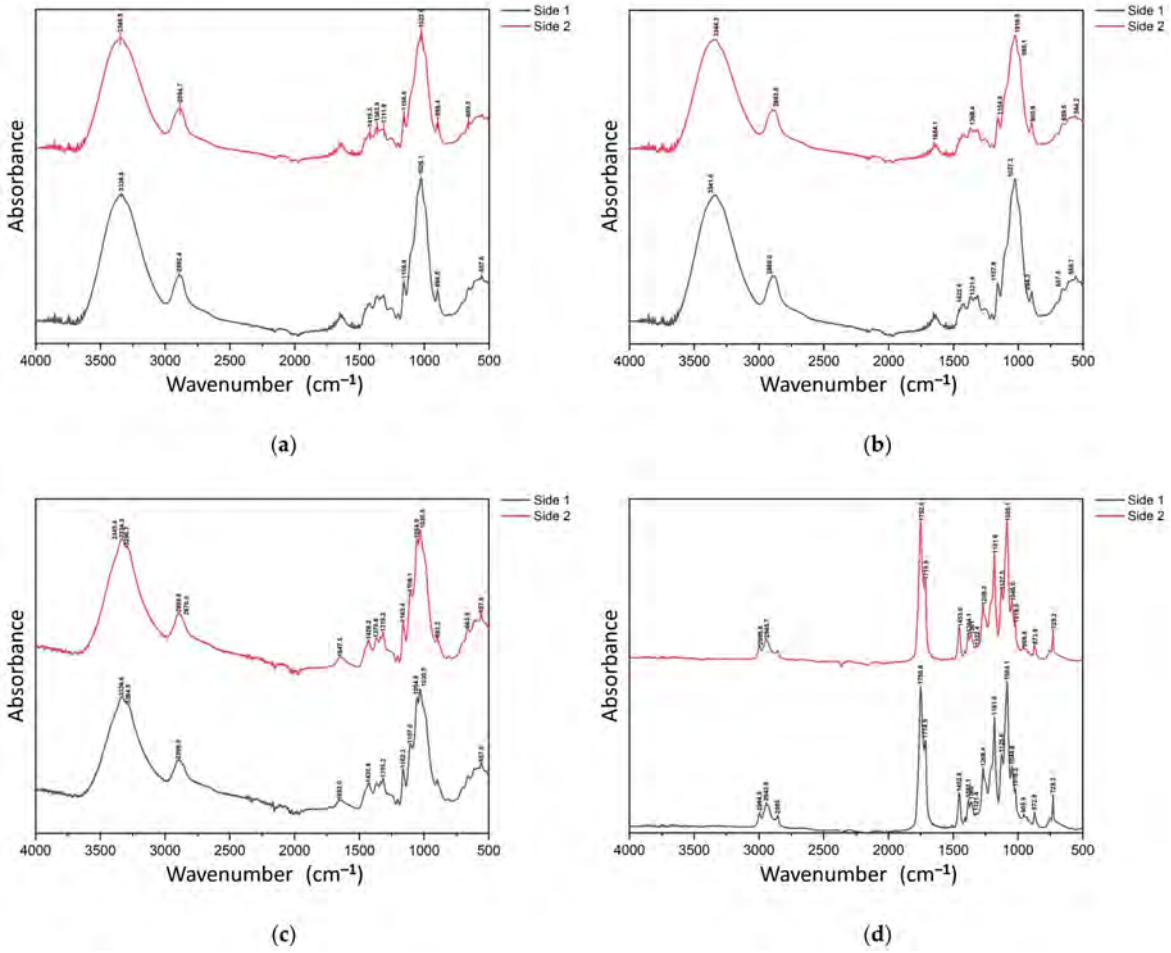

Figure 2. *Cont.*

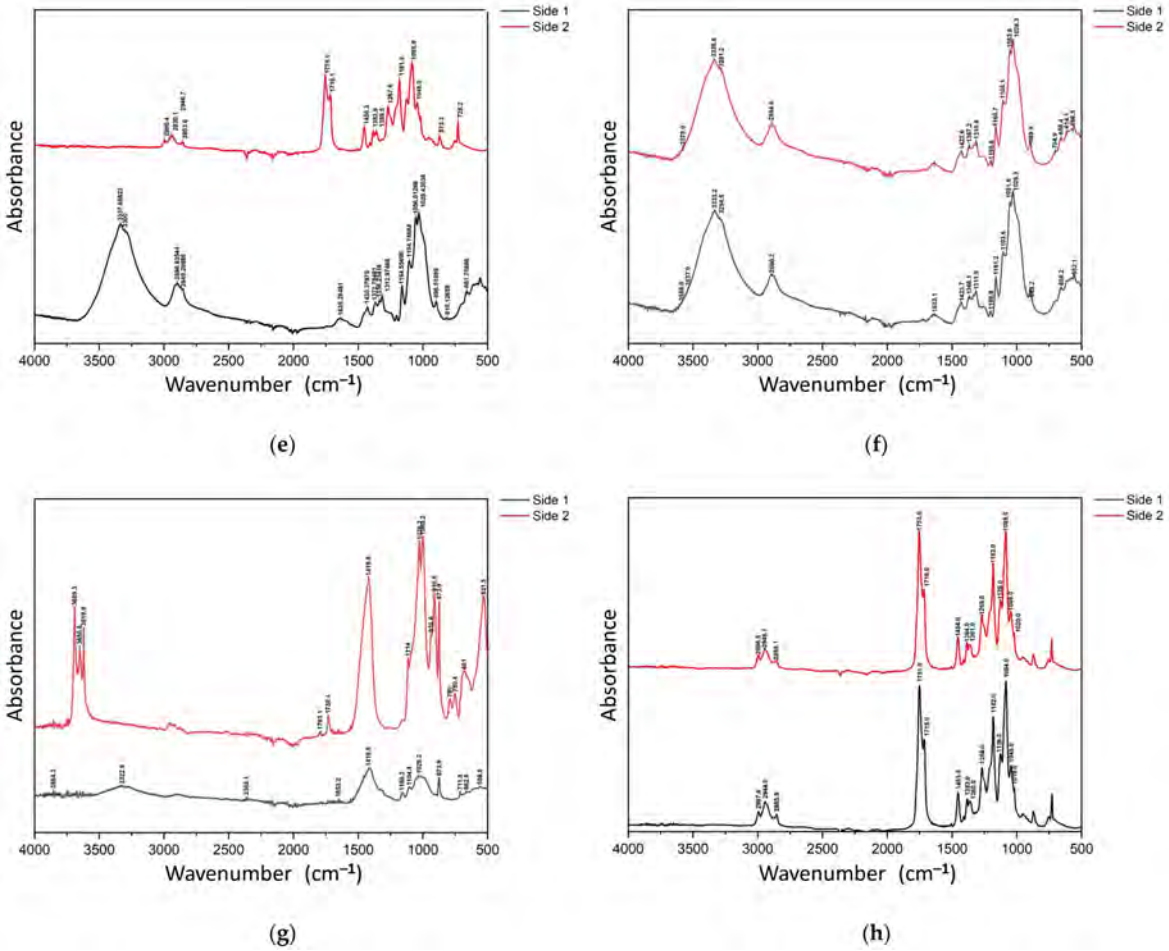

Figure 2. Fourier-transform infrared spectra of biopolymers; (**a**) Product 1; (**b**) Product 2; (**c**) Product 3; (**d**) Product 4; (**e**) Product 5; (**f**) Product 6; (**g**) Product 7; (**h**) Product 8.

FT-IR spectra of Product 1 shown in Figure 2a confirm that the polymer's chemical composition is based on cellulose derivatives. The acquired spectrum is comparable with those of other studies [50,51]. Both sides of the polymer film exhibited similar chemical composition. The functional groups of cellulose are recorded as peaks at 896 cm^{-1}, characteristic of β-glycosidic linkages between glucose units and at 3346 cm^{-1} representing –OH bond stretching. Absorption bands at 2892 and 1419 cm^{-1} are attributed to the stretching and bending of C–H bond. Furthermore, the peak observed at 1022 cm^{-1} is attributed to pyranose ring skeleton vibration. Characteristics of the plastics materials are shown in Tables 2 and 3. The VS content of Product 1 was 92.01%, and pH value was neutral (7.3); moreover, small amounts of Ca and Mg were detected in the cellulosic material, accounting for 0.1% dm and 0.04% dm, respectively, according to ICP-OE spectroscopy results.

Spectra of Products 2, 3, and 6 are shown in Figure 2b,c,f, respectively, and they all exhibited similar peaks. By comparing the obtained spectra with previous studies [52,53], it was found that these polymers are chemically composed of cellulose and calcium carbonate ($CaCO_3$) filler. Peaks around 1030 cm^{-1} can be attributed to C-O-C pyranose ring skeletal vibration of cellulose. The absorption band at 1434 cm^{-1} is characteristic of $v_{3\text{-}3}$ CO_3^{2-} and $v_{3\text{-}4}$ CO_3^{2-}; additionally, peaks around 670 cm^{-1} indicate the presence of calcite in the polymers' matrices. ICP-OE spectroscopy results showed that Ca content by dry mass percentage of Products 2, 3, and 6 was 2.3%, 3.2%, and 1.5%, respectively (Table 3). VS content was 88.3%, 73.9%, and 64.6%, respectively, for Products 2, 3, and 6.

FT-IR spectra of Product 4 are represented in Figure 2d. Both sides showed similar spectra. By comparing the acquired spectra with other studies [54–57], it can be concluded that the polymer's grade is based on PLA and PBAT blend. The location of the PLA/PBAT

characteristic peaks essentially mirrors the peaks of PLA and PBAT. The peaks at 1752, 2995, and 1084 cm^{-1} are assigned to the stretching vibrations C=O, CH_3 asymmetric and C-O which are attributed to PLA. In addition, ester vibration in PLA is reported at 872 cm^{-1}. C-H plane of benzene ring vibration in PBAT is recorded at 728 cm^{-1}. The peaks at 1715 cm^{-1} and 2945 cm^{-1} represent the stretching vibration of C-O, and CH_2, respectively in PBAT. The VS content of Product 4 was 99.1%.

Table 3. Results of the physicochemical characterization of the plastics and inoculum.

Plastics	Chemical Composition [a]	TS [a,b]	VS [a,b]	OM [a,b]	pH
		(% wm)			
Product 1	Cellulose or derivative(s)	92.81 ± 0.23 ^{AB}	92.01 ± 0.22 ^{A}	99.14 ± 0.20 ^{A}	7.3
Product 2	Cellulose or derivative(s) with $CaCO_3$	93.30 ± 0.22 ^{A}	88.32 ± 0.22 ^{B}	64.66 ± 0.18 ^{B}	7.2
Product 3	Cellulose or derivative(s) with $CaCO_3$	95.15 ± 0.28 ^{C}	73.86 ± 0.22 ^{C}	77.63 ± 0.20 ^{C}	7.0
Product 4	A blend of PLA and PBAT	99.16 ± 0.23 ^{D}	99.14 ± 0.17 ^{D}	99.98 ± 0.19 ^{D}	6.9
Product 5	The outer side contains cellulose or derivatives(s) and $CaCO_3$, the inner side is a blend of PLA and PBAT	95.92 ± 0.13 ^{E}	95.74 ± 0.26 ^{E}	99.82 ± 0.25 ^{D}	7.2
Product 6	Cellulose or derivative(s) with $CaCO_3$	94.45 ± 0.22 ^{F}	64.57 ± 0.25 ^{F}	68.37 ± 0.26 ^{E}	7.0
Product 7	Cellulose or derivative(s) with $CaCO_3$ and, kaolinite	92.54 ± 0.19 ^{B}	89.01 ± 0.23 ^{G}	96.19 ± 0.15 ^{F}	7.3
Product 8	Pure PLA	85.00 ± 0.26 ^{G}	82.73 ± 0.20 ^{H}	97.33 ± 0.20 ^{G}	6.8
Inoculum	Mesophilic inoculum	5.87 ± 0.24	4.73 ± 0.39	80.5 ± 8.1	7.9

[a] Abbreviation, chemical formula: $CaCO_3$—calcium carbonate; PLA—polylactic acid; PBAT—poly(butylene adipate terephthalate); TS—total solids; VS—volatile solids; OM—organic matter; wm—wet mass; [b] Different superscript capital letters indicate statistical significance ($p < 0.050$).

FT-IR spectra of Product 5 shown in Figure 2e obtained from both sides of the polymer film revealed different functional groups at the two sides. Side 1 depicted characteristic peaks of cellulose. The functional groups of cellulose are recorded as peaks at 896 cm^{-1}, characteristic of β-glycosidic linkages between glucose units, at 1029 cm^{-1}, which is attributed to C-O-C pyranose ring skeletal vibration of cellulose, and at 3337 cm^{-1}, representing –OH bond stretching [51,52], whereas Side 2 showed characteristic peaks of PLA/PBAT blend. The peaks at 1756, 2995, 1085.9 are assigned to the stretching vibrations C=O, CH3 asymmetric, C-O which are attributed to PLA. C-H plane of benzene ring vibration in PBAT is recorded at 728 cm^{-1}. The peaks at 1716 cm^{-1} and 2930 cm^{-1} represent the stretching vibration of C-O, and CH_2 in PBAT. Hence, Product 5 can be described as PLA/PBAT coated paper. VS content of Product 4 was 95.74% [55–57].

FT-IR spectra of Product 7 shown in Figure 2g obtained from both sides of the film exhibited different spectra. By comparing the acquired spectra with the previous studies [53,54], it can be confirmed that Side 1 is composed of cellulose with a calcium carbonate filler, whereas Side 2, which visually appeared glossy, is coated with a mixture between calcium carbonate and kaolin. The spectrum representing Side 1 exhibited a peak at 1026 cm^{-1}, which can be attributed to the C-O-C pyranose ring skeletal vibration of cellulose. The absorption band at 1407 cm^{-1} is characteristic of $v_{3\text{-}3}$ CO_3^{2-} and $v_{3\text{-}4}$ CO_3^{2-}; additionally, the peak at 670 cm^{-1} indicates the presence of calcite in the polymer's matrix. On the other side, the characteristic peaks of kaolinite are recorded between 3500 cm^{-1} and 3700 cm^{-1} [57]. In addition, the absorption band at 1421.5 cm^{-1} is characteristic of $v_{3\text{-}3}$ CO_3^{2-} and $v_{3\text{-}4}$ CO_3^{2-}, and the peak at 676.6 cm^{-1} indicates the presence of calcite. VS content was 89.0%, the Ca content was 5.7% dm.

FT-IR spectra of Product 8 are shown in Figure 2h. The peaks at 1751, 2994, and 1084 cm^{-1} are assigned to the stretching vibration C=O, CH_3 asymmetric, and C-O, respectively, which are attributed to PLA. Besides these, ester vibration in PLA is reported at 872 cm^{-1}, and therefore, Product 8 is composed of pure PLA [54].

3.2. Statistical Analysis of the Results of the Elemental Analysis

The results of the elemental analysis, including the TS, Vs, OM, and pH values are found in Table 3. The values are presented as the averages of three replicate measurements in every case with the indicated standard deviation (SD) values. The significant differences between the investigated bioplastic materials are indicated according to the detected values for each parameter.

According to the results, significant differences were observed in the measured parameters during the statistical comparisons of the investigated bioplastic materials. The highest TS values were observed for Product 4 (99.16 ± 0.23%) ($p < 0.001$), while the lowest TS was determined for Product 8 (85.00 ± 0.26%) ($p < 0.001$). Products 2, 3, and 6 were characterized with the same composition (cellulose/cellulose derivatives and calcium carbonate), but in the TS values, significant differences were observed despite the same composition ($p \leq 0.025$). Between Product 1 and Product 2, a significant difference was not detected ($p = 0.203$); moreover, Product 1 and Product 7 are statistically also identical based on the determined TS values ($p = 0.799$). In the PLA-containing Products (Products 4, 5, and 8), significant differences were demonstrated as well ($p < 0.001$).

In the case of the VS values, significant differences were determined between all groups ($p < 0.001$). The highest values were detected for Product 4 (99.14 ± 0.17% wm), similarly in the case of the measured TS values, while the lowest VS values were determined for Product 6 (64.57 ± 0.25% wm). Since significant differences were determined between all groups, groups characterized by the same composition (Products 2, 3, and 6—cellulose/cellulose derivatives and calcium carbonate; Products 4, 5, and 8—PLA-containing products) are also different ($p < 0.001$).

The highest OM values were determined for Product 4 (99.98 ± 0.19% wm) and Product 5 (99.82 ± 0.25% wm) compared to the other investigated bioplastic materials ($p \leq 0.016$), but between them, a significant difference was not proved ($p = 0.978$). The lowest OM was detected for Product 2 (64.66 ± 0.18% wm). Despite the compositional similarity, significantly higher OM was detected for Product 3 and Product 6 compared to Product 2 ($p < 0.001$). In the case of the PLA-containing products, significantly lower OM was observed for Product 8 (pure PLA) compared to Product 4 and Product 5 ($p < 0.001$).

The additional results of the elemental analysis, including the C, H, N, S, O, Ca, and Mg. ThBMP, and BD_{30} values are presented in Table 4. The values are presented as the averages of three replicate measurements in every case with the indicated standard deviation (SD) values. The percentages by dry mass of carbon, hydrogen, nitrogen, oxygen, and sulfur were used to calculate the ThBMP of each plastic.

The highest C content was observed for Product 4 (56.1 ± 0.20% dm) compared to the other investigated plastic product ($p < 0.001$), while the lowest values were detected for Product 7 (36.1 ± 0.20% dm) ($p < 0.001$). Significant differences were observed for Products 2, 3, and 6 despite the same characterized composition ($p < 0.001$), and this statement is also true for products containing PLA (Products 4, 5, and 8) ($p < 0.001$). However, significant differences between Products 1, 5, and 6 were not detected in C content values based on our measurements ($p \geq 0.491$).

Based on the H content values, the highest H content was observed for Product 4 (5.27 ± 0.21% dm), similarly in the case of the C content; however, significant differences were not demonstrated between Product 4 and the other groups ($p \geq 0.229$), except for Product 3 and Product 7 ($p < 0.001$). The lowest values were detected for Product 7 (4.15 ± 0.26% dm), but significant differences were not observed between Product 7 and the following products: Products 3 and 8 ($p \geq 0.051$). In contrast to the determined C content, in the case of the identical (Products 2, 3, and 6—cellulose/cellulose derivatives and calcium carbonate), and similar compositional characterized (PLA-containing products—Products 4, 5, and 8), products significant differences were not observed ($p \geq 0.062$).

Table 4. Results of the elemental analysis. The percentages by dry mass of carbon, hydrogen, nitrogen, oxygen, and sulfur were used to calculate the theoretical biomethane potential of each plastic product.

Plastic	C [a,b]	H	N	S	O	Ca	Mg	ThBMP	BMP	BD_{30}
	(% dm)							(NmL/gVS)	(NmL/gVS)	(%)
Product 1	45.5 ± 0.2^{A}	4.98 ± 0.23^{A}	0.013 ± 0.008^{A}	0.130 ± 0.005^{A}	41.6 ± 0.2^{A}	0.041 ± 0.001^{A}	0.137 ± 0.007^{A}	453.2 ± 9.6^{A}	432.6 ± 1.1^{A}	95 ± 12^{A}
Product 2	43.2 ± 0.3^{B}	4.86 ± 0.16^{AB}	0.073 ± 0.007^{B}	0.022 ± 0.006^{B}	42.3 ± 0.1^{B}	0.053 ± 0.001^{B}	2.262 ± 0.006^{B}	431.8 ± 6.1^{A}	437.1 ± 1.0^{A}	101 ± 6^{A}
Product 3	37.4 ± 0.2^{C}	4.24 ± 0.21^{BC}	0.024 ± 0.008^{AC}	0.041 ± 0.005^{CD}	35.5 ± 0.1^{C}	0.079 ± 0.002^{C}	3.191 ± 0.006^{C}	444.0 ± 12.3^{A}	327.2 ± 0.6^{B}	74 ± 6^{B}
Product 4	56.1 ± 0.2^{D}	5.27 ± 0.21^{A}	0.059 ± 0.006^{D}	0.004 ± 0.001^{E}	38.2 ± 0.2^{D}	0.018 ± 0.002^{D}	0.055 ± 0.004^{D}	538.6 ± 8.7^{B}	114.1 ± 0.9^{C}	23 ± 6^{C}
Product 5	45.9 ± 0.2^{A}	4.90 ± 0.27^{A}	0.056 ± 0.003^{DE}	0.055 ± 0.001^{C}	37.8 ± 0.2^{DE}	0.029 ± 0.002^{E}	1.086 ± 0.004^{E}	487.2 ± 10.3^{C}	266.2 ± 3.3^{D}	55 ± 3^{D}
Product 6	45.8 ± 0.2^{A}	4.84 ± 0.24^{AB}	0.028 ± 0.005^{AC}	0.053 ± 0.001^{CD}	37.4 ± 0.2^{E}	0.033 ± 0.001^{E}	1.474 ± 0.009^{F}	489.8 ± 10.6^{C}	310.9 ± 0.3^{E}	63 ± 3^{BD}
Product 7	36.1 ± 0.2^{E}	4.15 ± 0.26^{C}	0.036 ± 0.007^{CD}	0.044 ± 0.001^{D}	33.9 ± 0.3^{F}	0.053 ± 0.002^{B}	5.694 ± 0.006^{G}	450.2 ± 13.2^{A}	266.4 ± 0.1^{D}	59 ± 4^{BD}
Product 8	49.7 ± 0.3^{F}	4.79 ± 0.22^{ABC}	0.010 ± 0.002^{A}	0.002 ± 0.001^{E}	45.1 ± 0.1^{G}	0.014 ± 0.002^{F}	0.048 ± 0.006^{D}	441.6 ± 8.3^{A}	50.4 ± 2.1^{F}	12 ± 2^{C}

[a] Abbreviation, chemical formula: C—carbon content; H—hydrogen content; N—nitrogen content; S—sulfur content; O—oxygen content; Ca—calcium content; Mg—magnesium content; ThBMP—theoretical biomethane potential; BD_{30}—biodegradability rate after 30 days; dm—dry mass; NmL/gVS—normalized mL volume of methane accumulated per gram mass of the volatile solid organic substance in the sample; [b] Different superscript capital letters indicate statistical significance ($p < 0.050$).

The highest N content was detected for Product 2 (0.073 ± 0.007% dm) compared to the other investigated bioplastic materials ($p \leq 0.026$). Therefore, we detected significantly lower N content for the other two products (Products 3 and 6) characterized by the identical composition compared to Product 2 ($p < 0.001$), but between Products 3 and 6, significant differences were not observed ($p = 0.998$). The lowest N values were measured for Product 8 (0.010 ± 0.002% dm), although significant differences were not detected between Product 8 and the following products: Products 1, 3, and 6 ($p \geq 0.086$). During the comparison of the PLA-containing products, significantly higher N content was detected for Products 4 and 5 compared to Product 8 ($p < 0.001$), but Products 4 and 5 were statistically identical according to the measured values ($p = 0.998$).

Based on the analysis of S contents, the obviously highest values were detected for Product 1 (0.130 ± 0.005% dm) ($p < 0.001$), while the lowest S contents were determined for Product 4 (0.004 ± 0.001% dm) and Product 8 (0.002 ± 0.001% dm), with both groups containing PLA and not being statistically different compared to each other ($p = 1.000$). For the third PLA-containing product (Product 5), significantly higher S content was determined compared to Products 4 and 8 ($p < 0.001$). Significant difference between Products 3 and 6 characterized by the same composition was not detected ($p = 0.511$), but for Product 2, with the same composition, a significantly lower S content was determined compared to Products 3 and 6 ($p < 0.001$).

The highest O content was detected for Product 8 (45.1 ± 0.14% dm) compared to the other investigated plastic products ($p < 0.001$). Compared to Product 8 (pure PLA), significantly lower O contents were measured for the other two PLA-containing Products 4 and 5 ($p < 0.001$), but between Products 4 and 5 significant difference was not demonstrated ($p = 0.351$). The lowest O content was observed for Product 7 (33.9 ± 0.26% dm) compared to the other groups ($p < 0.001$), similarly in the case of the C and H contents. A significant difference was observed between Products 2, 3, and 6 despite the same compositional characteristics ($p < 0.001$).

The higher Ca content was measured for Product 3 (0.079 ± 0.002% dm) compared to the other investigated plastic products ($p < 0.001$), while the lower Ca content was detected for Product 8 (0.014 ± 0.002% dm), similarly in the case of the S content. In the case of Products 2, 3, and 6 characterized by the same composition, compared to Product 3 with the highest Ca content, significantly lower Ca values were observed for Products 2 and 6 ($p < 0.001$), and there was significant difference also between Products 2 and 6 ($p < 0.001$). Moreover, significant differences were detected among all products containing PLA ($p < 0.001$).

Based on the detected Mg content values, the highest content was observed for Product 7 (5.694 ± 0.006% dm) compared to the other investigated bioplastic materials ($p < 0.001$). The lowest Mg contents were determined for Product 4 (0.055 ± 0.004% dm) and Product 8 (0.048 ± 0.006% dm), with both products containing PLA; in addition, Products 4 and 8 are statistically identical ($p = 0.934$). For the third PLA-containing product, Product 5, significantly higher Mg content was demonstrated compared to the other two products containing PLA ($p < 0.001$). Furthermore, statistically significant differences were demonstrated between Products 2, 3, and 6 despite the same compositional characteristics (cellulose/cellulose derivatives and calcium carbonate) compared to each other ($p < 0.001$).

Significant differences were also detected in the calculated ThBMP between the investigated bioplastic materials. The highest ThBMP was observed for PLA-containing Product 4 (538.6 ± 8.7 NmL/gVS) compared to the other groups ($p < 0.001$). Furthermore, the highest C- and H contents were observed also for Product 4. Significant differences were observed between the other two products containing PLA (Products 5 and 8) ($p = 0.001$). The lowest calculated ThBMP values were detected for Product 2 (431.8 ± 6.1 NmL/gVS), but significant differences were not demonstrated between Product 2 and the following products: Product 1, 3, 7, and 8 ($p \geq 0.842$). However, Products 2 and 3 are statistically and compositional the same ($p = 0.807$), and the ThBMP of Product 6 is significantly higher

compared to Products 2 and 3 with the same composition (cellulose/cellulose derivatives and calcium carbonate) based on the analysis ($p < 0.001$).

The significant differences between the investigated bioplastic materials are indicated in Table 3 according to the detected values for each parameter.

3.3. Theoretical Methane (ThBMP) Production and Biomethane Potential (BMP) Test

The BMP of the 8 investigated biodegradable plastics in the study, under mesophilic anaerobic conditions, and the development of biomethane production are represented in Figures 3 and 4, respectively. BMP was characterized by measured values at the end of the BMP tests (on the 30th day). Significant differences were recorded between BMP values according to the chemical composition of the polymers (Figure 2). The average of the BMP values ranged between 50.4 ± 2.1 NmL/gVS (Product 8) and 437.5 ± 1.0 NmL/gVS (Product 2). Based on the statistical analysis, the lowest BMP was detected for Product 8, containing PLA, compared to the other groups ($p < 0.001$). In Products 4 and 5, partly containing PLA, significantly higher BMP was detected compared to the pure-PLA Product 8 ($p < 0.001$), and significantly higher BMP was observed for Product 5 compared to Product 4 ($p < 0.001$). Based on the results the BMP for PLA-containing products is highly affected by the presence of the other components (e.g., PBAT and cellulose/cellulose derivatives). The highest BMP values were detected for Product 1 (432.6 ± 1.1 NmL/gVS) and Product 2 (437.5 ± 1.0 NmL/gVS) compared to the other investigated plastic products ($p < 0.001$), and there was no significant difference between Products 1 and 2 ($p = 0.533$). According to the results of the elemental analysis Products 2, 3, and 6 were characterized by the same composition (cellulose/cellulose derivatives and calcium carbonate), but based on the statistical analysis, significant differences were detected despite the same composition. During the comparisons of Products 2, 3, and 6, the significantly highest BMP was detected for Product 2 (437.5 ± 1.0 NmL/gVS) compared to Products 3 and 6 ($p < 0.001$); moreover, significantly higher BMP was detected for Product 3 compared to Product 6 ($p < 0.001$). Significant differences between the products with the same identified composition indicates that additional parameters also affect the BMP. The BMP determined for Product 7 (characterized composition: cellulose/cellulose derivatives, calcium carbonate, and kaolinite) was statistically identical to Product 5 ($p = 1.000$). According to the BMP tests, Product 1 and Product 2 have the most favorable BMP characteristic, while the lowest BMP was detected for Product 8. In contrast to ThBMP, the highest BD_{30} values were detected for Product 2 (431.8 ± 6.1%) compared to the other groups ($p < 0.001$) except for Product 1 ($p = 0.910$). In the case of Products 2, 3, and 6, characterized by the same composition, there was no significant difference between Product 3 and Product 6 ($p = 0.425$). The lowest BD_{30} values were observed for Product 8 (12 ± 2%), similarly in the case of S-, Ca-, and Mg contents, but there was no significant difference between PLA-containing Products 8 and 4 ($p = 0.382$). Significantly higher BD_{30} was determined for Product 5, also containing PLA, compared to Product 4 and Product 8 ($p < 0.001$).

Based on the BMP curves, the amount of produced methane can be characterized every single day according to the measurements in the three parallels. The BMP curves show the average of the three measured values with the standard deviation. BMP curves generally can be characterized by a short initial linear phase between the first five days; however, for Products 1 and 2, the initial linear phase was even shorter (Figure 4). Gradiation values of the initial phase of BMP curves can be viewed in Table 5. We found a significant relationship ($p < 0.001$) between the time (days) and BMP values ($R^2 = 0.899–0.964$) during the initial phase.

During the additional statistical analysis of the BMP curves, polynomial regression fittings (second, third, and fourth orders) were performed on certain curves. Based on the quantitative parameters (e.g., p value, R^2, and Akaike Information Criterion (AIC)), different orders were fitted on BMP curves. According to the results of polynomial regression third-order regression was applied for Products 2, 6, and 8, while for the other products (Products

1, 3, 4, 5, and 7), the fourth-order fitting was appropriate (Table 6). Based on the elemental analysis, Products 2 and 6 were characterized by the same composition.

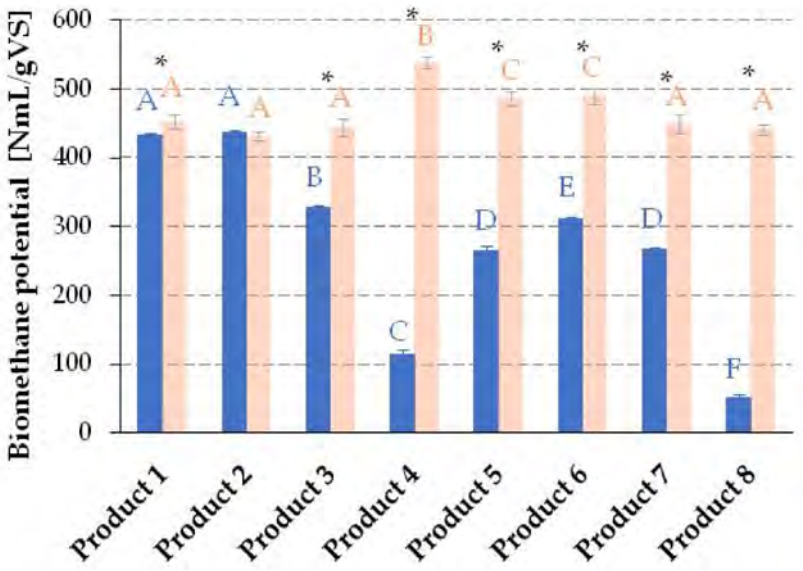

Figure 3. Average biomethane potential (BMP) (blue columns) and theoretical methane production (ThBMP) (orange columns) of the biodegradable plastics used in the study on the 30th day of the experiment. Different letters indicate significant differences in BMP (blue) and ThBMP (orange) between the investigated products ($p < 0.05$). Asterisks (*) indicate significant differences between the BMP and ThBMP for the given product (Product 1: $p = 0.021$, Products 3–8: $p < 0.001$).

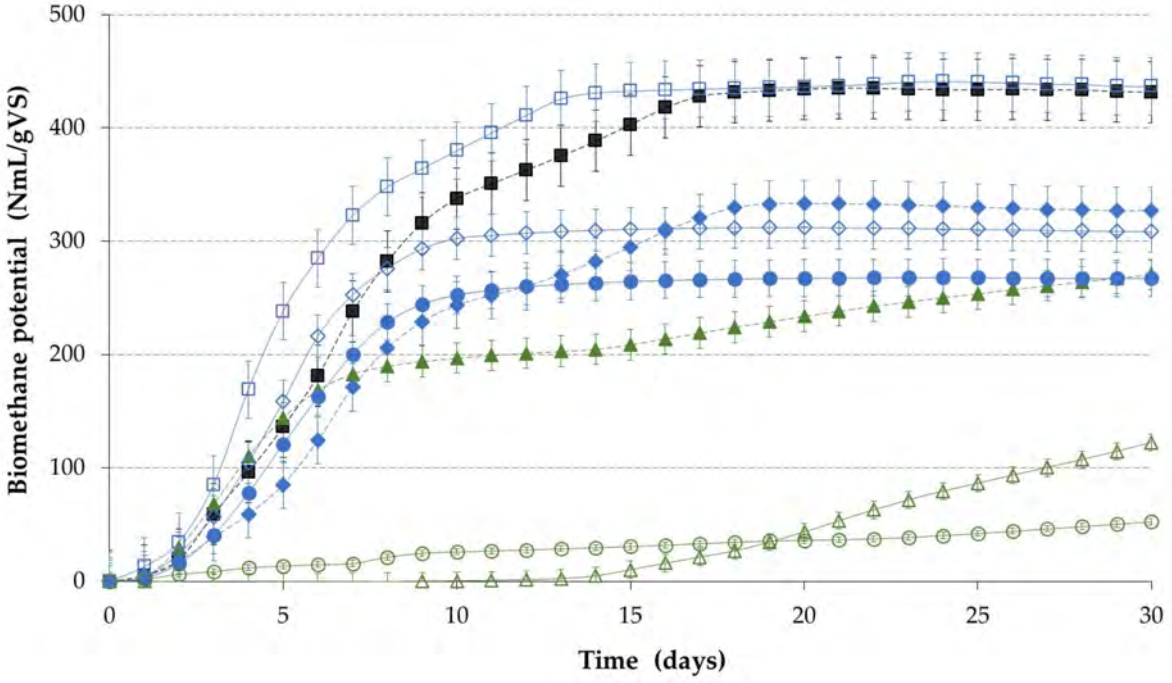

Figure 4. Assessment of the biomethane potential of the eight biodegradable plastics (Products 1 to 8) used in the study on the basis of methane (CH_4) development under anaerobic digestion conditions. Product 1 (■, black dashed line), Product 2 (□, blue solid line), Product 3 (⧫, blue dashed line), Product 4 (△, green solid line), Product 5 (▲, green dashed line), Product 6 (◊, blue solid line), Product 7 (●, blue solid line), Product 8 (o, green solid line).

Table 5. Gradiation values of the initial phase of BMP curves based on the results of linear regression.

Plastic	Slope	Y Intercept	R^2	*p* Value
Product 1	9.51	−1.46	0.920	<0.001
Product 2	9.10	−1.16	0.936	<0.001
Product 3	17.4	−8.86	0.956	<0.001
Product 4	0.907	0.114	0.964	<0.001
Product 5	30.7	−17.8	0.950	<0.001
Product 6	32.4	−22.4	0.915	<0.001
Product 7	24.4	−18.0	0.899	<0.001
Product 8	2.61	−1.65	0.908	<0.001

Table 6. Data of polynomial regression tests accomplished on the BMP curves. Values in bold indicate the best fitting model.

Plastic	Order 1			Order 2			Order 3		
	p Value	R^2	AIC	*p* Value	R^2	AIC	*p* Value	R^2	AIC
Product 1	<0.001	0.917	974.5	<0.001	0.920	971.9	**<0.001**	**0.924**	**967.4**
Product 2	<0.001	0.932	937.7	**<0.001**	**0.973**	**854.7**	<0.001	0.972	856.5
Product 3	<0.001	0.975	805.5	<0.001	0.976	805.1	**<0.001**	**0.981**	**781.6**
Product 4	<0.001	0.902	754.1	<0.001	0.901	755.4	**<0.001**	**0.908**	**750.0**
Product 5	<0.001	0.899	858.0	<0.001	0.958	777.4	**<0.001**	**0.968**	**752.2**
Product 6	<0.001	0.900	917.2	**<0.001**	**0.962**	**829.0**	<0.001	0.961	830.6
Product 7	<0.001	0.909	883.1	<0.001	0.953	821.0	**<0.001**	**0.954**	**819.7**
Product 8	<0.001	0.881	572.6	**<0.001**	**0.894**	**562.7**	<0.001	0.893	564.0

Based on the result of Gompertz modeling, mostly the applied Gompertz-type models well fitted our measured BMP values, although for PLA-containing products (Products 4, 5, and 8) the Gompertz models were not suitable for the prediction and estimation of BMP. This phenomenon is explained by the lack of reaching the second, declining phase of methane production within the 30-day test period, and therefore, the Gompertz models do not become convergent and are not able to properly predict the upper plateau. The fact that the duration of the test highly affects the prediction accuracy of Gompertz models is known in the scientific literature [30]. Therefore, in the case of the PLA-containing Products 4, 5, and 8, a longer test duration would be required for the Gompertz model to be applicable.

The determined coefficients A, B, and C originated from the Gompertz equation, as well as the resulting modified Gompertz model fitting data for the maximum specific BMP (A), maximum specific methane production rate (μm), and the length of the lag phase (λ); moreover the calculated R^2 values are presented in Table 7. The percentage deviations between the measured and predicted BMP values according to Gompertz models are also summarized in Table 7.

According to the calculated R^2 values, Gompertz models fitted our measured BMP values perfectly in case of the Products 1, 2, 3, 6, and 7, while the determined R^2 values were $\geq$0.995. After the fitting of the models, the lowest differences between the experimental and estimated values were detected for Products 2 and 7 (0.2%), while the highest deviation (1,4 and 1.5%) was determined for Product 3. Based on the highest estimated and also the related measured BMP values suggesting that Products 1 and 2 can be characterized with the highest potential for biogas production. The larger values of coefficient C indicate a faster rate of BMP growth for Products 2 and 6, while a slower BMP growth rate for Product 3 can be predicted by the Gompertz models. Based on the output parameters of modified Gompertz models, the highest maximum specific methane production rate was observed for Product 2 (170.7), while the lowest was calculated in case of Products 3 and 5. According to the estimated lag phases, the longest time taken to produce biogas was observed for Products 1 and 3 (5.4–5.8 days), while the shortest lag-phase was estimated for Product 5 (3.6 days) according to the modified Gompartz model (Table 7). The lag

phase correlated with the hydrolysis rate, thus short lag phase indicating shorter hydrolysis phase resulting reduced growth rate, while longer lag phase and hydrolysis phase resulting reduced growth rate [58].

Table 7. The coefficients and parameters of the applied traditional and modified Gompertz models accomplished on the BMP values.

Plastic	BMP	Gompertz Model					Modified Gompertz Model				
	Exp. [a,b]	Coef. a [c]	Coef. b [d]	Coef. c [e]	R^2	% Dev [f]	A [g]	μm [h]	λ [i]	R^2	% Dev
	(NmL/gVS)			(NmL/gVS/day)			(NmL/gVS)	(NmL/gVS/day)	(day)		
Product 1	432.6 ± 1.1 [A]	436.0	1.762	126.7	0.998	0.8	435.2	46.86	5.442	0.998	0.6
Product 2	437.1 ± 1.0 [A]	437.4	1.182	169.2	0.998	0.0	436.8	62.68	4.023	0.997	0.2
Product 3	327.2 ± 0.6 [B]	332.3	1.860	88.76	0.995	1.5	331.7	32.85	5.837	0.995	1.4
Product 4	114.1 ± 0.9 [C]	– [j]	–	–	–	–	–	–	–	–	–
Product 5	266.2 ± 3.3 [D]	–	–	–	–	–	–	–	–	–	–
Product 6	310.9 ± 0.3 [E]	313.6	2.287	164.3	0.999	0.9	313.8	60.07	4.097	0.999	0.9
Product 7	266.4 ± 0.1 [D]	266.8	2.413	128.0	0.999	0.1	266.9	46.90	4.423	0.999	0.2
Product 8	50.4 ± 2.1 [F]	–	–	–	–	–	–	–	–	–	–

[a] the experimental BMP; [b] different superscript capital letters indicate statistical significance ($p < 0.050$); [c] coefficient a—estimated maximum BMP; [d] coefficient b—shift along the time axis (analogous to the lag phase); [e] coefficient c—slope at the infection point of the curve; [f] % deviation between the experimental and estimated BMP values; [g] estimated maximum BMP; [h] maximum specific methane production rate; [i] lag phase; [j] convergence not achieved in the Gompartz models to the experimental data (for Product 4, 5 and 8).

Product 1 (cellulosic polymer) and Product 2 (cellulose and calcium carbonate filler) exhibited similar behaviors and were readily biodegradable with no lag phase. Biomethane production was intensive with fast kinetics. The degradation plateau was reached in less than 16 days in the case of Product 1 and less than 20 days in the case of Product 2. For Product 1, during the first ($p < 0.001$) and second week ($p < 0.001$) the BMP values were significantly higher compared to the initial values. From the second week, the determined BMP values for Product 1 showed no further significant changes ($p \geq 0.760$). Based on the statistical comparisons of BMP values, the same significant continuous growth of BMP values was observed for Product 2 during the first two weeks ($p < 0.001$), and after the initial phase, in the detected BMP values significant differences were not observed until the end of the test ($p \geq 0.984$). The biomethane production at the end of the 30-day experiment were 432.6 ± 1,1 NmL/gVS and 437.5 ± 1.0 NmL/gVS for Products 1 and 2, respectively, corresponding to a methane conversion of 95 ± 12% and 101 ± 6% for Products 1 and 2.

Similarly, Product 3 (cellulose and calcium carbonate) was readily biodegradable with no lag phase. The biogas production was intensive in the first 10 days of the experiment then slowed down slightly until reaching the plateau on day 21. Compared to Products 1 and 2, the continuous significant growth of BMP values was observed not only until the second but also the third week ($p < 0.010$), but after reaching the plateau, significant differences were not detected in the measured BMP values ($p = 0.986$). The BMP was 327.2 ± 0.6 NmL/gVS by the end of the 30-day test period, corresponding to methane conversion of 74 ± 6%. This value is lower than the one recorded in the case of Product 2, although, chemical analysis revealed that both products have similar chemical compositions, this difference may be attributed to the lower content of TS and VS in Product 3.

Product 4 showed a long lag phase of about 15 days. After the lag phase, biomethane production started with slow kinetics, without reaching a biodegradation plateau within the 30-day test period. During the observed lag phase and the first 15–21 days significant differences in the detected BMP values were not detected ($p \geq 0.135$). Compared to the initial BMP values significantly higher BMP values were determined on the fourth week ($p = 0.010$), and the continuous growth of BMP values was observed until the end of the BMP test. By the end of the experiment, the BMP was 114.09 ± 7.47 NmL/gVS conforming to 23 ± 6% methane conversion.

Product 5 started the AD process with almost no lag phase (< 1 day). The methane production was intensive in the first 9 days of the experiment. After that, the kinetics of

the biodegradation declined and a steady increase in methane production was observed until completion within 30 days. Significantly higher BMP values were determined one week later ($p < 0.001$) compared to the initial values, and the continuous growth of BMP values was also observed until the 30th day at the end of the BMP test, although, similarly to Product 4. The total evolved biomethane volume by the end of the experiment was 266.17 ± 3.30 NmL/gVS corresponding to 55 ± 3% methane conversion. Based on the determined BMP values for Product 6, continuous and significant growth of BMP values was observed during the first two weeks ($p < 0.001$). After the second week, a slight increase in BMP values was observed, but in the detected BMP values between the 3rd and 4th weeks significant differences were not demonstrated ($p = 0.997$). By the end of the experiment, BMP was 310.9 ± 0.3 NmL/gVS.

Similarly, the BMP of Product 7 kicked off in less than 1 day from the beginning of the experiment with fast kinetics until the 7th day of the test when BMP values reached a biodegradation plateau. During the first two weeks, the continuous increase in BMP values was observed compared to the initial values ($p < 0.001$). After the second week, a slight growth of the values was demonstrated, but in the detected BMP values between the 2nd and 5th weeks, significant differences were not detected ($p \geq 0.994$). The cumulative BMP by the end of the test was 266.4 ± 0.1 NmL/gVS corresponding to 59 ± 4% biomethane conversion.

Product 8 exhibited slow kinetics without exhibiting a biodegradation plateau. During the BMP tests, based on the weekly measured BMP values, the continuous and slow growth of BMP values was detected. Compared to the initial values, the detected BMP values were significantly higher every week ($p \leq 0.033$). The maximum experimental biomethane production was 50.4 ± 2.1 NmL/gVS with a 12 ± 2% conversion rate.

Based on the comparisons of the weekly determined BMP values for the different investigated bioplastic materials, one week later, the highest BMP values were detected for Product 2 compared to the other products ($p \leq 0.012$), while the lowest BMP values were determined for Products 4 and 8 ($p < 0.001$), and statistical differences between the two group was not observed ($p = 0.970$). In the case of Products 2, 3, and 6 characterized by the same chemical composition (cellulose/cellulose derivatives and calcium carbonate), significant differences were detected between the groups ($p \leq 0.002$) despite the same composition. During the comparison of PLA-containing products, as above mentioned, statistical differences between Products 4 and 8 were not observed ($p = 0.970$), but for Product 5 significantly higher BMP was detected compared to the other two products containing PLA ($p < 0.001$).

On the 2nd week, the highest BMP values were observed for Products 1 and 2 ($p \leq 0.015$), while the lowest BMP values were also detected for Products 4 and 8 ($p < 0.001$), between the groups with the maximum and minimum values significant differences were not demonstrated, respectively ($p \geq 0.365$). In contrast to the 1st week, between groups characterized by the same chemical composition, significant differences in the determined BMP values were not observed between Products 3 and 6 ($p = 0.752$), but for Product 2 significantly higher BMP was evaluated compared to Products 3 and 6 ($p < 0.001$). In the case of products containing PLA (Products 4, 5, and 8) the observed differences and tendencies were the same as those observed in the first week.

From the 3rd week to the 4th week, the highest BMP values were observed also for Products 1 and 2 ($p < 0.001$), while the lowest values were still typical for Products 4 and 8 ($p < 0.001$) compared to the other groups. Furthermore, the observed differences between groups characterized by the same chemical composition (Products 2, 3, and 8—cellulose/cellulose derivatives and calcium carbonate) were not modified from the 2nd week until the end of the test period ($p < 0.05$). In the case of products containing PLA, no further differences were observed compared to the above presented differences between Products 4, 5, and 8.

During the statistical analysis and comparisons of the BMP values, generally, the significant effects of time and the chemical composition were observed on the BMP values

($p < 0.001$); moreover, the interaction of the two factors was also statistically significant based on our measurements ($p < 0.001$).

4. Conclusions

Regarding the cellulose-based biopolymers, the generated results can be compared with other studies found in the literature [30,59–62]. El-Mashad et al. [59] found that BMP tests on sugar cane bagasse based plates and Kraft paper, resulted in 507 NmL/gVS and 133 NmL/gVS, respectively. The BMP values of different cellulose-based products (miscellaneous paper, newspaper used for wrapping kitchen waste, used paper, waste high-quality paper, and paper garbage bag) investigated by Kobayashi et al. [60], were 380, 360, 430, 570, and 260 NmL/gVS, respectively. Calabrò et al. [30] measured the biomethane produced by cellulosic plates under mesophilic conditions (35 ± 0.5 °C). The results showed that the cumulative biomethane production after 44 days was 311 ± 37.6 NmL/gVS, indicating a full degradation of the plates (99.9 ± 0.03% mass reduction). Furthermore, BMP tests performed by Dolci et al. [61] on bags made of recycled paper manufactured for food waste collection resulted in 272 ± 7 NmL/gVS under mesophilic conditions and 262 ± 6 NmL/gVS under thermophilic conditions, suggesting that this product is highly degradable under both conditions. The composition of the feed materials in terms of carbohydrate, fat, and protein content has a direct impact on methane generation and composition. Moreover, physical and chemical properties of the substrate employed, such as pH, moisture content, total and volatile solids (VS), particle size, and biodegradability, all play an important role in the anaerobic digestion process and further in methane production. Cellulose is a renewable carbon source that is composed entirely of glucose units and is degraded by extracellular enzymes secreted by the microorganisms. Fungi such as Trichoderma, Penicillium, and Fusarium spp. are effective cellulolytic enzyme producers [14]. As previously mentioned, the AD process can be divided into four distinguished processes: hydrolysis, acidogenesis, acetogenesis, and methanogenesis. Hydrolysis is the principal mechanism by which enzymes degrade cellulose polymers. Extracellular enzymes perform the first stages of depolymerization outside of the microbial cells. After cleavage, the smaller oligomers can be transferred into cells for final mineralization where the final product is a biogas mixture of mainly CH_4 and CO_2. Hence, cellulose-based products readily biodegrade with fast kinetics in AD processes [61]. Furthermore, the replacement of different types of substituents for the hydroxyl groups on the cellulose backbone results in a diverse spectrum of cellulose derivatives with varying characteristics which may increase its biodegradability [61]. Hence, it can be concluded that cellulose-based materials can convert efficiently under mesophilic conditions into methane, at a relatively short retention time; hence, they can be regarded as a promising material for co-digestion with feedstock in AD digesters. Finally, the methane production varies with regard to the VS content and specific chemical composition of the cellulose-based products (cellulose and additives content).

The results of pure PLA degradation are similar to those obtained in the literature [62–64]. Bernat et al. [62] investigated the anaerobic biodegradation of PLA (plastic cup) at 58 °C and 37 °C and found that the maximal biogas production was achieved in 40 and 280 days under thermophilic and mesophilic conditions, respectively. Moreover, the biogas production was 1.5 times higher under thermophilic conditions. A similar study conducted by Vasmara and Marcheti [63] showed that biodegradation of PLA did not occur in 90 days at 35 °C; however, at 55 °C the BMP of PLA was 282 NmL/gVS. Hence, the biodegradation of pure PLA is enhanced under thermophilic conditions as the hydrolysis of the material is more successful when there is a variety of biomass present, and microorganism accessibility to the substance is probably improved by the material's molecular structure degrading at high temperatures. On the other hand, thermo-alkaline pretreatment of PLA, involving solubilization via treatment with 5% calcium hydroxide at 70 to 90 °C temperatures, prior to anaerobic degradation under mesophilic conditions was found to be an effective method to improve its BMP [64].

There are a limited number of studies that investigated the biodegradation behavior and BMP of PLA/PBAT blends. It is important to highlight that the results obtained from these studies vary significantly, which is probably due to the variation of the experimental setups and the unknown specific composition of the tested biopolymers [4]. Peng et al. [65] examined the biodegradation of PLA/PBAT-based biopolymer bags under mesophilic and thermophilic AD. The results revealed that the biomethane production recorded from both digesters incubating the polymer with inoculum and the blank (inoculum only) by the end of the test was 90 NmL/gVS. Similar results were found under thermophilic conditions, where both digesters containing the polymer and the inoculum and the blank produced around 33 NmL/gVS, suggesting that the biodegradation of this polymer did not occur under both conditions. Furthermore, Ren et al. [66] investigated the biodegradation behavior of PLA, PBAT, and their blends under mesophilic AD. The results revealed that the rate of PLA biodegradation is 8.6%, while the rate of PBAT biodegradation is 5.9%. Blending the two polymers resulted in an increase in the overall crystallinity of the composite material, suggesting that PBAT may cause PLA to develop a new crystal structure; however, the FT-IR results showed that the macromolecular chain breaks down during the degradation process confirming that the biodegradation has occurred. In contrast, the BMP results of bioplastic bags commercialized as Mater-Bi®, which is a starch-based material with a composition of 70% PBAT, 20% starch, and 10% additives [61], ranged between 56.5 ± 0.4 and 86.1 ± 15.1 under mesophilic conditions. BMP results of PLA/PBAT under mesophilic AD investigated by Fernandes et al. [67], were around 25 NmL/gVS, deducing that PLA/PBAT was vulnerable to microbial attack, probably because it contains a large content of aliphatic polyesters. Additionally, in the aliphatic block of PBAT, scission could happen, but not close to the benzene ring. In our study, the lag phase observed in the curve representing the BMP in NmL/gVS of Product 4) (PLA/PBAT blend) (Figure 3) exhibited a long lag phase, which is probably due to the presence of complex compounds found in the blend, resulting in slow initial breakdown of the larger molecules. Furthermore, the characteristics crystalline structure of the blend can slow down the hydrolysis phase at the beginning of the AD process [68,69]. After hydrolysis, the degradation of monomers by microorganisms proceeds, which can explain the increase in BMP value in Product 4 after the lag phase. The BMP value by the end of the test was high compared to the previously mentioned studies; therefore, further analyses are required to investigate the ratio of PLA to PBAT in the blend and other chemical composition that cannot be revealed through surface spectroscopy analysis and can greatly influence the biodegradation process. By the end of the test, the methane conversion was BD_{30} = 22%. However, the hydraulic retention time for industrial AD plants is 21 days [70]; hence, under these mesophilic conditions, this blend is not regarded as a promising material for co-digestions with feedstock in industrial biogas plants.

According to the results of the elemental analysis and BMP test, in the determined values for the investigated parameters and BMP values for the commercial bioplastic materials analyzed, significant differences can be observed even in the case of the same or closely similar chemical compositions (Products 2, 3, and 6—cellulose/cellulose derivatives and calcium carbonate), and partially similar composition (PLA-containing products—Products 4, 5, and 8). Hence, the exact chemical composition of the additives and their biodegradation behavior should be studied by means of analytical methods as they may have a significant effect on the BMP of the bioplastics in which they are contained. Based on our results, the Gompertz models are suitable model to predict the rate and potential of biomethane production of the investigated bioplastic materials; however, for the PLA-containing Products 4, 5, and 8, the applied Gompertz models were not applicable presumably due to the short test duration. The most favorable BMP characteristics were detected for Products 1 and 2, while the lowest BMP was observed for Product 8 (pure PLA). Thus, it is apparent that BMP values are highly affected by the composition of the bioplastic materials. Based on the significant differences between the products with the same identified composition indicates that additional parameters also affect the BMP. According to our results, determined BMP

values for PLA-containing products are highly affected by the presence of the other components (e.g., PBAT and cellulose/cellulose derivatives). The significant effects of time and the chemical composition of the investigated bioplastics on the BMP values were observed; furthermore, their interaction was also significant with regard to BMP values. These data can be utilized to assist in defining operating parameters for anaerobic digesters when feedstocks including bioplastics enter AD plants. Furthermore, the results of the study revealed that cellulose-/cellulose derivate-based bioplastics produce high BMP values, and thus, they may provide added value to organic waste fraction management. The next steps of the research may involve evaluating the AD process at full scale concentrating on the behavior of different types of cellulose-/cellulose derivative-based products in terms of biodegradation and biogas production. Moreover, the results revealed that PLA-containing bioplastics had lower BMP values under anaerobic mesophilic conditions. The next steps of the research might involve testing the effect of mechanical, thermal, and chemico-thermal pre-treatment of these products on the BMP.

Author Contributions: Conceptualization, Z.Ü. and L.A.; methodology, Z.Ü.; validation, Z.V. and S.K.; formal analysis, M.D., S.K. and A.S.; investigation, Z.Ü., Z.V. and C.G.; writing—original draft preparation, M.D., M.W.R. and S.K.; writing—review and editing, G.F., Z.V., A.S. and L.A.; supervision, L.A.; funding acquisition, C.G. and L.A. All authors have read and agreed to the published version of the manuscript.

Funding: This research was funded by the Hungarian National Research, Development, and Innovation Office, project TKP2021-NVA-22, and project 2022-2.1.1-NL-2022-00006 "Development of the Agrotechnology National Laboratory" (Grant agreement NKFIH-3524-1/2022) supported from the National Research, Development and Innovation Fund by the Hungarian Ministry of Culture and Innovation, as well as by the Hungarian Ministry of Technology and Industry, project KEHOP-3.2.1-15-2021-00037.

Institutional Review Board Statement: Not applicable.

Informed Consent Statement: Not applicable.

Data Availability Statement: Not applicable.

Acknowledgments: The Authors express their sincere appreciation to the Forensic Institute of the National Tax and Customs Administration (Budapest, Hungary) for the analysis and for their expert contribution to this report, as well as to the Centre for Circular Economy Analysis and Knowledge founded by the Hungarian University of Agricultural and Life Sciences (MATE) for enrolling this project in its education profile.

Conflicts of Interest: The authors declare no conflict of interest.

References

1. European Bioplastics. Available online: https://www.european-bioplastics.org (accessed on 15 January 2023).
2. European Environment Agency (EEA). *Plastics, the Circular Economy and Europe's Environment*; EEA: Copenhagen, Denmark, 2021; Available online: https://www.eea.europa.eu/publications/plastics-the-circular-economy-and (accessed on 15 January 2023).
3. Lee, A.; Liew, M.S. Ecologically derived waste management of conventional plastics. *J. Mater. Cycles Waste Manag.* **2019**, *22*, 1–10. [CrossRef]
4. Cazaudehore, G.; Guyoneaud, R.; Evon, P.; Martin-Closas, L.; Pelacho, A.M.; Raynaud, C.; Monlau, F. Can anaerobic digestion be a suitable end-of-life scenario for biodegradable plastics? A critical review of the current situation, hurdles, and challenges. *Biotechnol. Adv.* **2022**, *56*, 107916. [CrossRef] [PubMed]
5. Folino, A.; Karageorgiou, A.; Calabrò, P.S.; Komilis, D. Biodegradation of wasted bioplastics in natural and industrial environments: A review. *Sustainability* **2020**, *12*, 6030. [CrossRef]
6. Abraham, A.; Park, H.; Choi, O.; Sang, B.I. Anaerobic co-digestion of bioplastics as a sustainable mode of waste management with improved energy production—A review. *Bioresour. Technol.* **2021**, *322*, 124537. [CrossRef]
7. Ahmed, T.; Shahid, M.; Azeem, F.; Rasul, I.; Shah, A.A.; Noman, M.; Hameed, A.; Manzoor, N.; Manzoor, I.; Muhammad, S. Biodegradation of plastics: Current scenario and future prospects for environmental safety. *Environ. Sci. Pollut. Res.* **2018**, *25*, 7287–7298. [CrossRef]
8. Polman, E.M.N.; Gruter, G.J.M.; Parsons, J.R.; Tietema, A. Comparison of the aerobic biodegradation of biopolymers and the corresponding bioplastics: A review. *Sci. Total Environ.* **2021**, *753*, 141953. [CrossRef]

9. Ali, S.S.; Elsamahy, T.; Abdelkarim, E.A.; Al-Tohamy, R.; Kornaros, M.; Ruiz, H.A.; Zhao, T.; Li, F.; Sun, J. Biowastes for biodegradable bioplastics production and end-of-life scenarios in circular bioeconomy and biorefinery concept. *Bioresour. Technol.* **2022**, *363*, 127869. [CrossRef]
10. Rabii, A.; Aldin, S.; Dahman, Y.; Elbeshbishy, E. A review on anaerobic co-digestion with a focus on the microbial populations and the effect of multi-stage digester configuration. *Energies* **2019**, *12*, 1106. [CrossRef]
11. Cazaudehore, G.; Monlau, F.; Gassie, C.; Lallement, A.; Guyoneaud, R. Methane production and active microbial communities during anaerobic digestion of three commercial biodegradable coffee capsules under mesophilic and thermophilic conditions. *Sci. Total Environ.* **2021**, *784*, 146972. [CrossRef]
12. Uveges, Z.S.; Ragoncza, Á.; Varga, Z.S.; Aleksza, L. Methane potential and respiration intensity of wastes and agricultural byproducts. *Appl. Ecol. Environ. Res.* **2020**, *18*, 6425–6441. [CrossRef]
13. Lü, F.; Wang, Z.; Zhang, H.; Shao, L.; He, P. Anaerobic digestion of organic waste: Recovery of value-added and inhibitory compounds from liquid fraction of digestate. *Bioresour. Technol.* **2021**, *333*, 125196. [CrossRef]
14. Cheng, J.J. (Ed.) Anaerobic digestion for biogas production. In *Biomass to Renewable Energy Processes*, 2nd ed.; CRC Press: Boca Raton, FL, USA, 2010; pp. 143–194.
15. Nguyen, L.N.; Nguyen, A.Q.; Nghiem, L.D. Microbial community in anaerobic digestion system: Progression in microbial ecology. In *Water and Wastewater Treatment Technologies. Energy, Environment, and Sustainability*; Bui, X.T., Chiemchaisri, C., Fujioka, T., Varjani, S., Eds.; Springer Nature: Singapore, 2019; pp. 331–355. [CrossRef]
16. Sahota, S.; Shah, G.; Ghosh, P.; Kapoor, R.; Sengupta, S.; Singh, P.; Vijay, V.; Sahay, A.; Vijay, V.K.; Thakur, I.S. Review of trends in biogas upgradation technologies and future perspectives. *Bioresour. Technol. Rep.* **2018**, *1*, 79–88. [CrossRef]
17. Kapoor, R.; Ghosh, P.; Tyagi, B.; Vijay, V.K.; Vijay, V.; Thakur, I.S.; Kamyab, H.; Nguyen, D.D.; Kumar, A. Advances in biogas valorization and utilization systems: A comprehensive review. *J. Clean. Prod.* **2020**, *273*, 123052. [CrossRef]
18. Alengebawy, A.; Mohamed, B.A.; Ghimire, N.; Jin, K.; Liu, T.; Samer, M.; Ai, P. Understanding the environmental impacts of biogas utilization for energy production through Life Cycle Assessment: An action towards reducing emissions. *Environ. Res.* **2022**, *213*, 113632. [CrossRef]
19. Adnan, A.I.; Ong, M.Y.; Nomanbhay, S.; Chew, K.W.; Show, P.L. Technologies for biogas upgrading to biomethane: A review. *Bioengineering* **2019**, *6*, 92. [CrossRef]
20. Samoraj, M.; Mironiuk, M.; Izydorczyk, G.; Witek-Krowiak, A.; Szopa, D.; Moustakas, K.; Chojnacka, K. The challenges and perspectives for anaerobic digestion of animal waste and fertilizer application of the digestate. *Chemosphere* **2022**, *295*, 133799. [CrossRef]
21. O'Connor, J.; Mickan, B.S.; Rinklebe, J.; Song, H.; Siddique, K.H.M.; Wang, H.; Kirkham, M.B.; Bolan, N.S. Environmental implications, potential value, and future of food-waste anaerobic digestate management: A review. *J. Environ. Manag.* **2022**, *318*, 115519. [CrossRef]
22. *EN 13432*; Packaging—Requirements for Packaging Recoverable through Composting and Biodegradation—Test Scheme and Evaluation Criteria for the Final Acceptance of Packaging. European Committee for Standardization: Brussels, Belgium, 2000.
23. *ISO 11734*; Water Quality—Evaluation of the "Ultimate" Anaerobic Biodegradability of Organic Compounds in Digested Sludge—Methods by Measurement of the Biogas Production. International Organization for Standardization: Geneva, Switzerland, 1995.
24. *ISO 14853*; Plastics—Determination of the Ultimate Anaerobic Biodegradation of Plastic Materials in an Aqueous System—Method by Measurement of Biogas Production. International Organization for Standardization: Geneva, Switzerland, 2016.
25. *ISO 15985*; Plastics—Determination of the Ultimate Anaerobic Biodegradation and Disintegration under High-Solids Anaerobic-Digestion Conditions—Method by Analysis of Released Biogas. International Organization for Standardization: Geneva, Switzerland, 2004.
26. *ASTM D5210-92*; Standard Test Method of Determining the Anaerobic Biodegradation of Plastic Materials in the Presence of Municipal sewage sludge. ASTM International: West Conshohocken, PA, USA, 2007.
27. *ASTM D5511-11*; Determining Anaerobic Biodegradation of Plastic Materials under High-Solids Anaerobic-Digestion Conditions. ASTM International: West Conshohocken, PA, USA, 2012.
28. *ASTM D5526-94D*; Determining Anaerobic Biodegradation of Plastic Materials under Accelerated Landfill Condition. ASTM International: West Conshohocken, PA, USA, 2018.
29. Ruggero, F.; Gori, R.; Lubello, C. Methodologies to assess biodegradation of bioplastics during aerobic composting and anaerobic digestion: A review. *Waste Manag. Res.* **2019**, *37*, 959–975. [CrossRef]
30. Calabrò, P.S.; Folino, A.; Fazzino, F.; Komilis, D. Preliminary evaluation of the anaerobic biodegradability of three biobased materials used for the production of disposable plastics. *J. Hazard. Mater.* **2020**, *390*, 121653. [CrossRef]
31. Calabrò, P.S.; Folino, A.; Maesano, M.; Pangallo, D.; Zema, D.A. Exploring the possibility to shorten the duration and reduce the number of replicates in biomethane potential tests (BMP). *Waste Biomass Valorization* 2022, *online first*. [CrossRef]
32. *MSZ EN 13040:2008*; Mass Determination. Hungarian Standards Institution: Budapest, Hungary, 2008. (In Hungarian)
33. American Public Health Association (APHA). *Standard Methods for the Examination of Water and Wastewater*, 21st ed.; APHA: Washington, DC, USA, 2005.
34. *MSZ EN 15935:2013*; Determination of Loss on Ignition. Hungarian Standards Institution: Budapest, Hungary, 2013. (In Hungarian)
35. *MSZ 13037:2012*; Determination of pH. Potentiometry. Hungarian Standards Institution: Budapest, Hungary, 2012. (In Hungarian)

36. *MSZ EN ISO 16948:2015*; Determination of Total Carbon, Hydrogen and Nitrogen Content. Hungarian Standards Institution: Budapest, Hungary, 2015. (In Hungarian)
37. *MSZ EN ISO 16994:2017*; Determination of Total Sulfur and Chlorine Content. Hungarian Standards Institution: Budapest, Hungary, 2017. (In Hungarian)
38. *MSZ 21470-50:2006*; Determination of Total and Soluble Toxic Element Content. Hungarian Standards Institution: Budapest, Hungary, 2006. (In Hungarian)
39. Boyle, W.C. Energy recovery from sanitary landfills—A review. In *Microbial Energy Conversion*; Schlegel, H.G., Barnea, J., Eds.; Pergamon Press: Oxford, UK, 1977; pp. 119–138. [CrossRef]
40. Raposo, F.; Fernández-Cegrí, V.; De La Rubia, M.A.; Borja, R.; Béline, F.; Cavinato, C.; Demirer, G.; Fernández, B.; Fernández-Polanco, M.; Frigon, J.-C.; et al. Biochemical methane potential (BMP) of solid organic substrates: Evaluation of anaerobic biodegradability using data from an international interlaboratory study. *J. Chem. Technol. Biotechnol.* **2011**, *86*, 1088–1098. [CrossRef]
41. Bioprocess Control Sweden. *AMPTS II & AMPTS II Light Automatic Methane Potential Test System, Version 3.0*; Bioprocess Control Sweden AB: Lund, Sweden, 2016.
42. The Association of German Engineers. *VDI 4630: Fermentation of Organic Materials—Characterisation of the Substrate, Sampling, Collection of Material Data, Fermentation Tests*; VDI Gesellschaft Energietechnik: Düsseldorf, Germany, 2006.
43. Krishania, M.; Vijay, V.K.; Chandra, R. Methane fermentation and kinetics of wheat straw pretreated substrates co-digested with cattle manure in batch assay. *Energy* **2013**, *57*, 359–367. [CrossRef]
44. Tjorve, K.M.C.; Tjorve, E. The use of Gompertz models in growth analyses, and new Gompertz-model approach: An addition to the Unified-Richards Family. *PLoS ONE* **2017**, *12*, e0178691. [CrossRef] [PubMed]
45. Ware, A.; Power, N. Modelling methane production kinetics of complex poultry slaughterhouse wastes using sigmoidal growth functions. *Renew. Energy* **2017**, *104*, 50–59. [CrossRef]
46. Pramanik, S.K.; Suja, F.B.; Porhemmat, M.; Pramanik, B.K. Performance and kinetic model of a single-stage anaerobic digestion system operated at different successive operating stages for the treatment of food waste. *Processes* **2019**, *7*, 600. [CrossRef]
47. Khedher, N.B.; Lattieff, F.A.; Mahdi, J.M.; Ghanim, M.S.; Majdi, H.S.; Jweeg, M.J.; Baazaoui, N. Modeling of biogas production and biodegradability of date palm fruit wastes with different moisture contents. *J. Clean. Prod.* **2022**, *375*, 134103. [CrossRef]
48. Buffington, D.E.; Jordan, K.A.; Boyd, L.L.; Junnila, W.A. Mathematical models of growth data of male and female Wrolstad white turkeys. *Poult. Sci.* **1973**, *52*, 1694–1700. [CrossRef]
49. Gomes, C.S.; Strangfeld, M.; Meyer, M. Diauxie studies in biogas production from gelatin and adaptation of the modified Gompertz Model: Two-phase Gompertz model. *Appl. Sci.* **2021**, *11*, 1067. [CrossRef]
50. Abderrahim, B.; Abderrahman, E.; Mohamed, A.; Fatima, T.; Abdesselam, T.; Krim, O. Kinetic thermal degradation of cellulose, polybutylene succinate and a green composite: Comparative study. *World J. Environ. Eng.* **2015**, *3*, 95–110. [CrossRef]
51. Chen, W.; He, H.; Zhu, H.; Cheng, M.; Li, Y.; Wang, S. Thermo-responsive cellulose-based material with switchable wettability for controllable oil/water separation. *Polymers* **2018**, *10*, 592. [CrossRef]
52. Ma, M.G.; Fu, L.H.; Li, S.M.; Zhang, X.M.; Sun, R.C.; Dai, Y.D. Hydrothermal synthesis and characterization of wood powder/$CaCO_3$ composites. *Carbohydr. Polym.* **2012**, *88*, 1470–1475. [CrossRef]
53. He, Q.; Huang, Z.; Liu, Y.; Chen, W.; Xu, T. Template-directed one-step synthesis of flowerlike porous carbonated hydroxyapatite spheres. *Mater. Lett.* **2007**, *61*, 141–143. [CrossRef]
54. Weng, Y.X.; Jin, Y.J.; Meng, Q.Y.; Wang, L.; Zhang, M.; Wang, Y.Z. Biodegradation behavior of poly(butylene adipate-co-terephthalate) (PBAT), poly(lactic acid) (PLA), and their blend under soil conditions. *Polym. Test.* **2013**, *32*, 918–926. [CrossRef]
55. França, D.C.; Almeida, T.G.; Abels, G.; Canedo, E.L.; Carvalho, L.H.; Wellen, R.M.R.; Haag, K.; Koschek, K. Tailoring PBAT/PLA/Babassu films for suitability of agriculture mulch application. *J. Nat. Fibers* **2018**, *16*, 933–943. [CrossRef]
56. Parameswaran, P.; Rittmann, E. Feasibility of anaerobic co-digestion of pig waste and paper sludge. *Bioresour. Technol.* **2012**, *124*, 163–168. [CrossRef]
57. Scaffaro, R.; Maio, A.; Gammino, M.; La Mantia, F.P. Effect of an organoclay on the photochemical transformations of a PBAT/PLA blend and morpho-chemical features of crosslinked networks. *Polym. Degrad. Stab.* **2021**, *187*, 109549. [CrossRef]
58. Tironi, A.; Trezza, M.; Irassar, E.; Scian, A. Thermal treatment of kaolin: Effect on the pozzolanic activity. *Procedia Mater. Sci.* **2012**, *1*, 343–350. [CrossRef]
59. El-Mashad, M.H.; Ruihong Zhang, R.; Greene, J.P. Anaerobic biodegradability of selected biodegradable plastics and biobased products. *J. Environ. Sci. Eng. A* **2012**, *1*, 108–114.
60. Kobayashi, T.; Xu, K.Q.; Li, Y.Y.; Inamori, Y. Evaluation of hydrogen and methane production from municipal solid wastes with different compositions of fat, protein, cellulosic materials, and the other carbohydrates. *Int. J. Hydrogen Energy* **2012**, *37*, 15711–15718. [CrossRef]
61. Dolci, G.; Catenacci, A.; Malpei, F.; Grosso, M. Effect of paper vs. bioplastic bags on food waste collection and processing. *Waste Biomass Valorization* **2021**, *12*, 6293–6307. [CrossRef]
62. Bernat, K.; Kulikowska, D.; Wojnowska-Baryła, I.; Zaborowska, M.; Pasieczna-Patkowska, S. Thermophilic and mesophilic biogas production from PLA-based materials: Possibilities and limitations. *Waste Manag.* **2021**, *119*, 295–305. [CrossRef] [PubMed]
63. Vasmara, C.; Marchetti, R. Biogas production from biodegradable bioplastics. *Environ. Eng. Manag. J.* **2016**, *15*, 2041–2048. [CrossRef]

64. Cazaudehore, G.; Guyoneaud, R.; Vasmara, C.; Greuet, P.; Gastaldi, E.; Marchetti, R.; Leonardi, F.; Turon, R.; Monlau, F. Impact of mechanical and thermo-chemical pretreatments to enhance anaerobic digestion of poly(lactic acid). *Chemosphere* **2022**, *297*, 133986. [CrossRef] [PubMed]
65. Peng, W.; Wang, Z.; Shu, Y.; Lü, F.; Zhang, H.; Shao, L.; He, P. Fate of a biobased polymer via high-solid anaerobic co-digestion with food waste and following aerobic treatment: Insights on changes of polymer physicochemical properties and the role of microbial and fungal communities. *Bioresour. Technol.* **2022**, *343*, 126079. [CrossRef]
66. Ren, Y.; Hu, J.; Yang, M.; Weng, Y. Biodegradation behavior of poly(lactic acid) (PLA), poly(butylene adipate-co-terephthalate) (PBAT), and their blends under digested sludge conditions. *J. Polym. Environ.* **2019**, *27*, 2784–2792. [CrossRef]
67. Fernandes, T.M.; De Almeida, J.F.; Escócio, V.A.; Da Silva, A.L.; De Sousa, A.M.; Visconte, L.L.; Leite, M.C. Evaluation of rheological behavior, anaerobic and thermal degradation, and lifetime prediction of polylactide/poly(butylene adipate-co-terephthalate)/powdered nitrile rubber blends. *Polym. Bull.* **2018**, *76*, 2899–2913. [CrossRef]
68. Arruda, L.C.; Magaton, M.; Bretas, R.E.S.; Ueki, M.M. Influence of chain extender on mechanical, thermal and morphological properties of blown films of PLA/PBAT blends. *Polym. Test.* **2015**, *43*, 27–37. [CrossRef]
69. Jiang, L.; Wolcott, M.P.; Zhang, J. Study of biodegradable polylactide/poly(butylene adipate-co-terephthalate) blends. *Biomacromolecules* **2005**, *7*, 199–207. [CrossRef]
70. Shrestha, A.; van-Eerten Jansen, M.C.; Acharya, B. Biodegradation of bioplastic using anaerobic digestion at retention time as per industrial biogas plant and international norms. *Sustainability* **2020**, *12*, 4231. [CrossRef]